Oxidation of hexacyanoferrate(II) ion by hydrogen peroxide: evidences of free radical intermediacy

Joaquin F. Perez-Benito [iD] · **Josep Pages-Rebull**

Joaquin F. Perez-Benito

jfperezdebenito@ub.edu

ORCID [iD]

J. F. Perez-Benito: 0000-0001-8407-3458

Departamento de Ciencia de Materiales y Quimica Fisica, Seccion de Quimica Fisica, Facultad de Quimica, Universidad de Barcelona, Marti i Franques 1, 08028 Barcelona, Spain

Abstract

The redox reaction between hexacyanoferrate(II) ion as the reducing agent and hydrogen peroxide as the oxidizing one, in slightly acid (pH 4.36 – 6.65) aqueous solutions containing phosphate ions, has been studied by means of an UV-Vis spectrophotometer monitoring the formation of Fe(III) at 420 nm. The initial hydrolysis of the Fe(II)-cyanide complex reactant to yield a pentacyanoaquaferrate(II) intermediate, as well as an increase in the solution pH (acid catalysis), had both a positive effect on the reaction rate, whereas an increase in the concentrations of Fe(III), phosphate and chloride ions, and D-mannitol had a negative effect (inhibition). A computer program, specifically designed for this purpose, allowed arriving at a complex eight-coefficient experimental rate law by application of the initial rate method, accounting for the dependences of the reaction rate on the concentrations of Fe(II), H_2O_2 and Fe(III). The reaction was characterized by a low value of the apparent activation energy (28.9 ± 2.7 kJ mol^{-1}) and a very negative value of the activation entropy (– 165 ± 9 J K^{-1} mol^{-1}). Finally, a multi-step reaction mechanism, involving the participation of a penta-coordinated Fe(II) *c*omplex and three free radicals (hydroperoxyl, superoxide and hydroxyl) as intermediates, has been proposed. This mechanism was supported by the available experimental information and confirmed by numerical simulations performed via the fourth-order Runge-Kutta integration method.

Keywords Free radical intermediates · Hexacyanoferrate(II) ion · Hydrogen peroxide · Inhibition· Kinetics · Mechanism

,

Introduction

According to the free radical theory of aging [1], a plausible mechanism for this phenomenon involves the participation of oxygen-containing free radicals in the formation of deleterious defects that would progressively accumulate inside the cells of aerobic organisms. Other non-radical reactive oxygen species generated in the normal metabolism would include hydrogen peroxide.

The reduction of molecular oxygen to water follows the well-known half reaction:

$$O_2 + 4H^+ + 4e^- \longrightarrow 2H_2O \qquad (1)$$

However, it is estimated that around 2% of the oxygen consumed suffers a monoelectronic reduction instead [2 – 4], thus initiating the sequence:

$$O_2 \xrightarrow{e^-} O_2^{\bullet -} \xrightarrow[2H^+]{e^-} H_2O_2 \xrightarrow{e^-} HO^- + HO^\bullet \xrightarrow[2H^+]{e^-} 2H_2O \qquad (2)$$

and leading to the formation of three potentially damaging reactive oxygen species: superoxide ion, hydrogen peroxide and hydroxyl radical [5]. Among them, the latter, because of its role as an initiator of a cascade of deleterious chain reactions [6], is indeed the most harmful metabolite for aerobes, especially as far as DNA alteration is concerned [7, 8], and it may be implicated in aging, carcinogenesis and other degenerative diseases [9, 10].

Although the main chemical agents able to reduce hydrogen peroxide to hydroxyl radical under physiological conditions are thought to be transition-metal ions in their lower oxidation

states [11], especially Fe(II) and Cu(I) in their protein-bounded forms [12 – 14], some authors (belonging to the field of chemistry rather than to that of biology) have openly opposed this interpretation, favoring either an Fe(IV) or a Cu(III) non-radical mechanism instead [15 – 26]. This has resulted in a certain polemic, since other authors favor the hydroxyl-based mechanism [27 – 33]. The resolution of this question is indeed of some importance because, on the contrary, the very own free radical theory of aging would be under jeopardy.

Given that iron(II) and iron(III) salts are water insoluble in neutral media due to the precipitation of the corresponding hydroxides, the kinetic study of their reactions with hydrogen peroxide under biologically relevant conditions makes mandatory the use of adequate metal-ligand complexes as an alternative [34 – 38]. In particular, the oxidation of hexacyanoferrate(II) ion by hydrogen peroxide has previously received some attention, the analysis of its kinetic behavior having been reported to be considerably hampered by reproducibility problems [39]. Other authors have found a simple first-order dependence on the concentration of the reducing agent and a more complex (Michaelis-Menten-like) dependence on that of the oxidizing agent, as well as acid catalysis [40]. The finding that the hexacyanoferrate(II)-hydrogen peroxide mixtures cause the hydroxylation of the naturally-occurring aromatic oil guaiacol (*o*-methoxyphenol) seems to suggest the participation of hydroxyl radicals as reaction intermediates [41]. On the other hand, the reaction object of the present research has been reported to be complex enough to produce pH oscillations when carried out in water-acetonitrile mixtures under closed-system conditions [42], making the study of its kinetics particularly attractive.

Experimental

Materials and methods

All the experiments were done using as solvent water previously purified by deionization followed by treatment with a Millipore Synergy UV system (milli-Q quality, κ = 0.05 μS/cm at 25.0 ºC). The reactants required to carry out the redox reaction were potassium hexacyanoferrate(II) trihydrate, $K_4[Fe(CN)_6]\cdot 3H_2O$ (Merck), as reducing agent and hydrogen peroxide, H_2O_2 (Sigma-Aldrich), as oxidizing agent. Other chemicals used were potassium hexacyanoferrate(III), $K_3[Fe(CN)_6]$ (Merck), to study the autoinhibition caused by one of the reaction products, potassium dihydrogenphosphate, KH_2PO_4, and dipotassium hydrogenphosphate trihydrate, $K_2HPO_4\cdot 3H_2O$ (both Merck), to control the medium pH, potassium chloride, KCl (Merck), as an inert electrolyte to determine a potential ionic strength effect, and 1,2,3,4,5,6-hexanehexol, $CH_2OH\text{-}(CHOH)_4\text{-}CH_2OH$ (D-mannitol, Sigma-Aldrich), as a hydroxyl radical scavenger.

Instrumentation

The pH measurements were done by means of a Wave pH-meter, provided with a digital presentation until the second decimal figure (± 0.01 pH) and a combination electrode, calibrated with the aid of commercial buffers of known pH (4.00 and 7.00, Sigma-Aldrich). The temperature was kept constant by means of a thermostatic bath provided with a digital reading (± 0.1 ºC). The kinetic runs were followed measuring periodically the absorbances at 420 nm with a Shimadzu 160 A UV-Vis spectrophotometer (± 0.001 *A*), using glass cells of 1

cm optical path length. At that wavelength the electronic spectrum of one of the reaction products, $[Fe(CN)_6]^{3-}$, shows a maximum absorption peak ($\mathcal{E}$ = 1015 M^{-1} cm^{-1}) [43].

Kinetic experiments

The total volume of the reaction mixtures was fixed at a constant value in all the experiments (25 mL). The last reactant to be added (1 mL of the desired concentration) to a thermostated aqueous solution containing all the other required chemicals (24 mL) was the reducing agent, Fe(II). In order to minimize the experimental errors associated with the kinetic data, the wavelength used to monitor the reaction (420 nm) was chosen as that leading to a higher increment of the solution absorbance between the initial and final points. The absorbances were periodically measured (time interval: 10 s) during at least 16 minutes. In total, 143 kinetic runs were performed.

Resolving the reproducibility problems

The reaction between hexacyanoferrate(II) ion and hydrogen peroxide gave unusual problems of irreproducibility, situation that was clearly related to the hydrolysis of the initial complex [44], given that the initial rate depended on the time elapsed after preparation of its aqueous solution, as well as on the laboratory illumination conditions. This difficulty was resolved by preparing the Fe(II) aqueous solution right before its use in each kinetic run, employing to that end already thermostated pure water as solvent, and no artificial light was used in the room during that procedure. Moreover, the time required for the preparation was reduced (and systematized from one experiment to another) as much as possible. In this way, a typical experiment repeated three times led to a standard deviation for the initial rate of ± 2.9 %.

Results and discussion

Initial rate method

A striking observation was the unusual complexity of the absorbance-time plots for the hexacyanoferrate(II) ion-hydrogen peroxide reaction, where a dramatic slowing down was found right from the beginning of the process, more intense than would be expected for a pseudo-first order reaction and even more than for a pseudo-second order one, in spite of H_2O_2 being in large excess with respect to Fe(II).

Thus, the initial rate method was the preferred way for obtaining the kinetic data. In our case, a fourth degree polynomial fitting the absorbance data corresponding to the first 240 s of each kinetic run yielded good enough results, the magnitudes directly measured in the laboratory (absorbance-time data couples) being fitted to a polynomial function of the type:

$$A(420) = a_o + a_1 t + a_2 t^2 + a_3 t^3 + a_4 t^4 \qquad (3)$$

and leading to the following expression for the initial rate:

$$v_o = \left(\frac{d\left[\mathrm{Fe(III)}\right]}{dt} \right)_{t=0} = \frac{1}{\varepsilon l} \left(\frac{dA(420)}{dt} \right)_{t=0} = \frac{a_1}{\varepsilon l} \qquad (4)$$

Hydrolysis of hexacyanoferrate(II) ion

The initial rate of the hexacyanoferrate(II)-peroxide reaction showed a strong dependence on the time elapsed after the preparation of the $K_4[Fe(CN)_6]$ stock solution, with a rapid increase at the beginning followed by a slow decrease afterwards (Fig. 1).

This finding is consistent with the involvement of two competitive reactions in the absence of H_2O_2. One of them is the hydrolysis of hexacyanoferrate(II) ion, $[Fe(CN)_6]^{4-}$, to yield pentacyanoaquaferrate(II) ion, $[Fe(CN)_5(H_2O)]^{3-}$. Provided that the latter is the actual active reducing agent for H_2O_2, this would explain the increase in the initial rate. The other is the oxidation of $[Fe(CN)_6]^{4-}$ by dissolved O_2 to yield $[Fe(CN)_6]^{3-}$ (a potential inhibitor of the $[Fe(CN)_6]^{4-} + H_2O_2$ reaction), which would explain the decrease in the initial rate after the maximum. Extrapolation of the initial rate at time zero, corresponding to the instant at which the stock Fe(II) aqueous solution was prepared, led to the value $v_o / [Fe(CN)_6^{4-}]_o[H_2O_2]_o = (5.3 \pm 1.7) \times 10^{-3}$ M^{-1} s^{-1} for the reaction of H_2O_2 with fresh, non-hydrolyzed $[Fe(CN)_6]^{4-}$ at 25.0 ºC (Fig. 1, inset). At the maximum of the initial rate vs. time plot the value of that ratio had increased by a factor of 20, meaning that the hydrolyzed complex reacts with hydrogen peroxide much faster than the non-hydrolyzed one.

The reversible hydrolysis of $[Fe(CN)_6]^{4-}$ follows the overall stoichiometry:

$$[Fe^{II}(CN)_6]^{4-} + H_3O^+ \underset{k_{-1}}{\overset{k_1}{\rightleftharpoons}} [Fe^{II}(CN)_5(H_2O)]^{3-} + HCN \qquad (5)$$

and its most probable mechanism consists of a three-step sequence of elementary reactions:

$$[Fe^{II}(CN)_6]^{4-} + H^+ \underset{k_{-2}}{\overset{k_2}{\rightleftharpoons}} [Fe^{II}(CN)_5(HCN)]^{3-} \quad (6)$$

$$[Fe^{II}(CN)_5(HCN)]^{3-} \underset{k_{-3}}{\overset{k_3}{\rightleftharpoons}} [Fe^{II}(CN)_5]^{3-} + HCN \quad (7)$$

$$[Fe^{II}(CN)_5]^{3-} + H_2O \underset{k_{-4}}{\overset{k_4}{\rightleftharpoons}} [Fe^{II}(CN)_5(H_2O)]^{3-} \quad (8)$$

This mechanism is coherent with the well-known property of hexacyanoferrates to release toxic hydrogen cyanide in strongly acidic media [45]. The reason should be looked for in the property of neutral molecules (such as HCN or H_2O) to be released from the cationic metal center of a complex more easily than anionic ligands (such as CN^-) do. Further, this can also explain why the hydrolyzed complex, pentacyanoaquaferrate(II) ion, reacts with H_2O_2 better than the non-hydrolyzed one, suggesting that the penta-coordinated ion formed in Eq. 7 has an important role as an intermediate, not only in the hydrolysis reaction, but also in the oxidation by hydrogen peroxide. This behavior is analogous to that observed in the complexation of the anti-tumor drug cisplatin with biological thiols, where replacement of a chloride ligand by water dramatically increases the reaction rate [46].

The corresponding rate law may be obtained by application of the quasi-equilibrium approximation to Eq. 6 (considered as a very fast reversible step) and that of the steady state to pentacyanoferrate(II) ion (considered as a very reactive intermediate present in minute concentration). This is equivalent to accept that the slow step is Eq. 7 in its forward direction, leading to the mathematical equation:

$$v_t = k_1 [Fe(CN)_6^{4-}]_t - k_{-1} [Fe(CN)_5(H_2O)^{3-}]_t [HCN]_t \quad (9)$$

where the rate constants for the forward and backward reactions in Eq. 5 are given by:

$$k_1 = \frac{K_2\, k_3\, k_4\, [H_3O^+]}{k_{-3}\, [HCN]_t + k_4\, [H_2O]} \quad (10)$$

$$k_{-1} = \frac{k_{-3}\, k_{-4}}{k_{-3}\, [HCN]_t + k_4\, [H_2O]} \quad (11)$$

As an approximation, since the concentration of HCN is indeed much smaller than that of water (997 g L^{-1}/18.015 g mol^{-1} = 55.3 M), it can be assumed that $k_{-3}\, [HCN]_t << k_4\, [H_2O]$, the integration leading then to the result [47]:

$$\ln \frac{c_o\, x_e + (c_o - x_e)\, x_t}{c_o\, (x_e - x_t)} = \frac{(2\, c_o - x_e)\, x_e}{c_o - x_e}\, k_{-1}\, t \quad (12)$$

where c_o is the initial concentration of $[Fe(CN)_6]^{4-}$, whereas x_t and x_e are the concentrations of $[Fe(CN)_5(H_2O)]^{3-}$ (as well as of HCN) at time t and once the equilibrium is reached, respectively. Equation 12 was applied by assuming that the values of x_t and x_e were directly proportional to the initial rates of the $[Fe(CN)_6]^{4-} + H_2O_2$ reaction (after addition of hydrogen peroxide) at time t ($v_{o,t}$) and at the maximum of the initial rate vs. time plot given in Fig. 1 ($v_{o,max}$), respectively, which is equivalent to accept that the $[Fe(CN)_6]^{4-} + H_2O_2$ redox reaction is of first order in the intermediate $[Fe(CN)_5(H_2O)]^{3-}$ formed in the hydrolysis reaction:

$$x_t = C\, v_{o,t} \quad ; \quad x_e = C\, v_{o,max} \tag{13}$$

where C is the proportionality constant required to replace the x values by those of v_o. From Eqs. 12 and 13 we infer:

$$\ln \frac{c_o\, v_{o,max} + (c_o - x_e)\, v_{o,t}}{c_o (v_{o,max} - v_{o,t})} = \frac{(2\, c_o - x_e)\, x_e}{c_o - x_e}\, k_{-1}\, t \tag{14}$$

Of the magnitudes appearing in the left-hand side of Eq. 14 the only one that is not directly available from the experimental data is x_e. The value of this magnitude was optimized so that the linearity of the ln $\{[c_o v_{o,max} + (c_o - x_e)\, v_{o,t}]/[c_o (v_{o,max} - v_{o,t})]\}$ vs. t plot was maximum.

From the slope of the corresponding linear plot (Fig. 2) and the value of x_e reached by optimization, the resulting rate constants for the hydrolysis reaction were k_1 = (1.3 ± 0.2) $\times 10^{-4}$ s^{-1} and k_{-1} = 0.21 ± 0.04 M^{-1} s^{-1}, yielding the equilibrium constant $K_1 = k_1/k_{-1}[H_3O^+]$ = (6.2 ± 2.1) $\times 10^3$ (at 25.0 ºC) and a maximum value for the hydrolysis degree of 29.7 %. The values so obtained were subject to a certain experimental error caused by the side reaction of oxidation of Fe(II) to Fe(III) with dissolved O_2. However, this error is probably of minor importance considering that the absolute value of the slope of the plot shown in Fig. 1 after the maximum is much lower than the slope before that maximum, when calculated at instants symmetrical with respect to that maximum. This means that the O_2–driven oxidation process happens at a rate much lower than the hydrolysis reaction.

The hydrolysis of hexacyanoferrate(II) ion is definitely a photochemical reaction [48], as made evident by the finding that, when the $K_4[Fe(CN)_6]$ stock solution was prepared and thermostated under ordinary laboratory-illumination conditions, its oxidation by H_2O_2 was much faster than when it was prepared and thermostated under semi-darkness conditions (Fig. 3). This feature is common with that presented by the photosensitive hydrolysis of hexacyanoferrate(III) ion [49, 50].

Kinetic data of the redox reaction

Five series of kinetic runs were performed at various initial concentrations of hydrogen peroxide, each of them consisting of five experiments differing in the initial concentration of hexacyanoferrate(II) ion, the other conditions remaining unchanged. The corresponding plots showed a downward-concave curvature at low $[H_2O_2]_o$ that slowly seemed to fade away as that concentration increased (Fig. 4, top). The same experiments allowed an analysis of the v_o vs. $[H_2O_2]_o$ dependence at different values of $[Fe(II)]_o$, leading to downward-concave curves in all five cases (Fig, 4, bottom).

In the presence of hexacyanoferrate(III) ion, the v_o vs. $[Fe(II)]_o$ plots showed first an upward-concave curvature followed by a downward-concave stretch (Fig. 5, top). On the other hand, the v_o vs. $[Fe(III)]_o$ plots showed a decreasing upward-concave pattern, indicating the existence of an autoinhibition effect caused by the oxidized complex formed as reaction product (Fig. 5, bottom).

As the concentration of KH_2PO_4 increased (the pH decreased) the initial rate first increased, passed through a maximum and then decreased (Fig. 6). These results should be

interpreted in terms of a combination of both acid catalysis (predominant a high pH values) and inhibition by phosphate ions (predominant a low pH values).

The Fe(II)-H_2O_2 reaction was also inhibited by both the apparently inert electrolyte potassium chloride (Fig.7, top) and the well-known hydroxyl radical scavenger D-mannitol (Fig. 7, bottom). The inhibition by KCl seemed to be too strong to be simply ascribed to an ionic strength effect.

The experimental kinetic data were coherent with both the Arrhenius (Fig. 8) and Eyring equations, leading to the values of the activation parameters listed in Table 1: the pre-exponential factor (A) and activation energy (E_a) from the Arrhenius model, and the entropy ($\Delta S^{\circ}_{\neq}$) and enthalpy ($\Delta H^{\circ}_{\neq}$) of activation from the Eyring model.

Experimental rate law

The laboratory results concerning the initial rate values obtained under different experimental conditions clearly pointed out to a rather complex kinetic equation. In order to get it, many trial mathematical functions were handled, and with each of them the percent error between the theoretical and measured values of the initial rate was obtained for 45 kinetic experiments, including different combinations of $[Fe(II)]_o$, $[H_2O_2]_o$ and $[Fe(III)]_o$. As a general rule, the calculations indicated that the higher the number of involved parameters (N), the lower the associated error, approaching asymptotically a minimum when $N = 8$ (Fig. 9).

A flow chart summarizing some of the trial equations is shown in Scheme 1. For the sake of simplicity, the best option leading to the lowest error has been chosen for each number of

parameters involved in the rate law. Finally, we arrived to what can be considered as the closest to reality kinetic equation, approaching as much as possible to the experimental data:

$$v_o = \frac{\left(k_I + k_{II}\,[H_2O_2]_o + k_{III}\,[Fe^{II}]_o\right)[Fe^{II}]_o\,[H_2O_2]_o + k_{IV}\,[Fe^{II}]_o^2}{\left(1 + k_V\,[Fe^{II}]_o + k_{VI}\,[Fe^{III}]_o\right)\left(1 + k_{VII}\,[Fe^{II}]_o + k_{VIII}\,[H_2O_2]_o\right)} \qquad (15)$$

The coefficients involved in all the tentative rate laws were optimized by means of a computer program, starting with some trial values and changing them systematically until the minimum error between the theoretical and experimental values of the initial rate was reached. For instance, in the case of the best 8-parameter law (Eq. 15) 1.21×10^8 different numerical combinations were required. The final values obtained for those coefficients, as well as their corresponding units, are compiled in Table 2.

Reaction mechanism

Given the complexity of the rate law obtained experimentally, it can be anticipated that a many-step mechanism will be required to explain it, probably involving the participation of free radicals as reaction intermediates. According to the available kinetic data, the best proposal we can offer is as follows:

$$[Fe^{II}(CN)_5(H_2O)]^{3-} \underset{k_{-5}}{\overset{k_5}{\rightleftharpoons}} [Fe^{II}(CN)_5]^{3-} + H_2O \qquad (16)$$

$$[Fe^{II}(CN)_5]^{3-} + CN^- \xrightarrow{k_6} [Fe^{II}(CN)_6]^{4-} \qquad (17)$$

$$[Fe^{II}(CN)_5]^{3-} + H_2O_2 \xrightarrow{k_7} [Fe^{II}(CN)_5(H_2O_2)]^{3-} \qquad (18)$$

$$[Fe^{II}(CN)_5]^{3-} + O_2 \xrightarrow{k_8} [Fe^{II}(CN)_5(O_2)]^{3-} \quad (19)$$

$$[Fe^{II}(CN)_5(H_2O_2)]^{3-} \xrightarrow{k_9} [Fe^{III}(CN)_4(C^{\bullet}(OH)N)(OH)]^{3-} \quad (20)$$

$$[Fe^{III}(CN)_4(C^{\bullet}(OH)N)(OH)]^{3-} + H_2O_2 \xrightarrow{k_{10}} [Fe^{III}(CN)_5(OH)]^{3-} + H_2O + HO_2^{\bullet} \quad (21)$$

$$HO_2^{\bullet} \underset{}{\overset{K_{11}}{\rightleftharpoons}} H^+ + O_2^{\bullet -} \quad (22)$$

$$[Fe^{II}(CN)_5(O_2)]^{3-} + CN^- \xrightarrow{k_{12}} [Fe^{III}(CN)_6]^{3-} + O_2^{\bullet -} \quad (23)$$

$$HO_2^{\bullet} + [Fe^{II}(CN)_6]^{4-} \xrightarrow[H^+]{k_{13}} H_2O_2 + [Fe^{III}(CN)_6]^{3-} \quad (24)$$

$$O_2^{\bullet -} + [Fe^{III}(CN)_6]^{3-} \xrightarrow{k_{14}} O_2 + [Fe^{II}(CN)_6]^{4-} \quad (25)$$

$$HO_2^{\bullet} + H_2O_2 \xrightarrow{k_{15}} O_2 + H_2O + HO^{\bullet} \quad (26)$$

$$HO^{\bullet} + [Fe^{II}(CN)_6]^{4-} \xrightarrow{k_{16}} HO^- + [Fe^{III}(CN)_6]^{3-} \quad (27)$$

$$O_2^{\bullet -} \xrightarrow{k_{17}} \text{wall} \quad (28)$$

The proposed mechanism starts with the hydrolyzed form of the reducing complex whose formation has been previously described in Eqs. 6-8. The loss of the water ligand from that high stability hexa-coordinated complex leads to a low stability, very reactive penta-coordinated complex (forward sense in Eq. 16), with a tendency to capture either a neutral molecule (such as H_2O, H_2O_2 or dissolved O_2) or a cyanide ion (coming from the complex hydrolysis, Eq. 7) as a sixth ligand (backward sense in Eq. 16 and Eqs. 17-19).

The capture of hydrogen peroxide as a ligand leads to the first redox step, where the transference of an electron from Fe(II) to the ligand results in the formation of Fe(III) and the lysis of the peroxide molecule into a hydroxide ion (that, because of its nature as a poor

leaving group [51], will remain bonded to the central metal ion) and a hydroxyl radical. Given that the experimentally observed activation energy (28.9 ± 2.7 kJ mol^{-1}, Table 1) was rather low for a reaction yielding hydroxyl radicals, we have opted for a concerted mechanism in which the electron transfer takes place simultaneously with the electrophilic addition of the emerging hydroxyl radical to a cyanide ligand to yield an organic free radical (Eq. 20). In fact, the addition reaction between free cyanide ion and the hydroxyl radical has previously been reported [52]. Moreover, an enhancement of the stability of the associated activated complex is expected by the electron-donating effect of the cyanide ligands. For instance, addition of L-cysteine decreases dramatically the activation energy of the Fe^{2+}/H_2O_2 Fenton reaction from 95.9 to 47.9 kJ mol^{-1} [53]. The organic free radical so formed may react with a second hydrogen peroxide molecule to give a hydroperoxyl radical (Eq. 21), and by a posterior dissociation a superoxide radical (Eq. 22). The corresponding acidity equilibrium constant is well known (pK_{11} = 4.69 at 25.0 ºC) [54].

On the other hand, the complex resulting from the replacement of a water molecule ligand by dissolved oxygen is unstable enough to yield (via an internal redox process) more Fe(III) and a superoxide ion radical (Eq. 23).

This intermediate may be found either in its protonated form (hydroperoxyl radical) or in its deprotonated one (superoxide ion) and, since the pH range of the present work was rather close to the pK_a of the former, both of them were present in similar concentrations. In addition, due to the differences in electron density, the electron-poor $HO_2^{\bullet}$ behaves as an oxidant in an Fe(II) → Fe(III) process (Eq. 24) and the electron-rich $O_2^{\bullet -}$ as a reductant in the opposite Fe(III) → Fe(II) process (Eq. 25), the latter thus explaining the autoinhibition provoked by the hexacyanoferrate(III) ion formed as reaction product.

Hydroperoxyl radical, as well as its deprotonated form (superoxide ion), may react with hydrogen peroxide to give a hydroxyl radical (Eq. 26). Although the existence of these reactions has often been put into question [55, 56], small but appreciable values (0.50 ± 0.09 M^{-1} s^{-1} for hydroperoxyl radical and 0.13 ± 0.07 M^{-1} s^{-1} for superoxide ion at 23.5 ºC) have been reported for their rate constants [57, 58]. The hydroxyl radical so formed is expected to react mainly with Fe(II) to yield more Fe(III) (Eq. 27).

Finally, it has been proposed that some of the hydroperoxyl/superoxide radicals may arrive at the reactor walls to disproportionate into O_2 and H_2O_2 on their surface (Eq. 28). Actually, an inhibiting surface effect has been reported for the Cu(II)/H_2O_2 reaction and explained in the same way [30].

Theoretical rate law

In order to compare the microscopic information contained in the mechanism with the macroscopic one gathered in the laboratory, it is necessary to deduce the theoretical rate law. For this purpose, the application of two different approximations, steady state and quasi-equilibrium [59, 60], was required. The first approximation can be applied only to short-lived, very reactive intermediates and was used to obtain the concentrations of the penta-coordinated complex (formed in Eq. 16), the Fe(II)-H_2O_2 complex (formed in Eq. 18), the Fe(II)-O_2 complex (formed in Eq. 19), the organic free radical (formed in Eq. 20), the hydroperoxyl radical (formed in Eq. 21), the superoxide ion radical (formed in Eqs. 22 and 23) and the hydroxyl radical (formed in Eq. 26). The second approximation can be applied only to very fast, reversible reactions, and this requirement was indeed fulfilled in the case of Eq. 22.

The theoretical rate law so deduced is consistent with the experimental one (Eq. 15), the macroscopic-microscopic relationships being those given in Table 3. Moreover, it can explain the observation of acid catalysis (increasing stretch in Fig. 6), since protonation of the superoxide ion radical favors the reaction ($Fe^{II} \rightarrow Fe^{III}$, Eq. 24) whereas deprotonation of the hydroperoxyl radical has the opposite effect ($Fe^{III} \rightarrow Fe^{II}$, Eq. 25). Notwithstanding, there is also an additional cause for the observed acid catalysis, given that a decrease of the pH results in a higher degree of hydrolysis of the initial Fe(II) complex (Eq. 5).

On the other hand, the inhibition by phosphate ions (decreasing stretch in Fig. 6), as well as that by chloride ion (Fig. 7, top), can be explained by a competition between either $H_2PO_4^-$ or Cl^- and H_2O_2 to fill the vacant position in the penta-coordinated Fe(II) complex formed in Eq. 16, although minor contributions due to ionic strength effects and reactions of those ions with the hydroxyl radical formed in Eq. 26 cannot be discarded (the reactions of both phosphate [61] and chloride [62] ions with that radical are well documented).

The initial rate decreased in the presence of the polyalcohol D-mannitol (Fig. 7, bottom). Since this natural sweetener of vegetable origin is a well-known specific hydroxyl radical scavenger [63, 64], its inhibitory effect may be taken as an experimental proof of the participation of that strongly oxidizing radical as a reaction intermediate.

Numerical simulations

The proposed mechanism has been obtained from laboratory measurements extrapolated to $t = 0$. In order to check its validity at other instants during the course of the reaction, the experimental rate law (Eq. 15) was integrated by an approximate numerical procedure known

as the fourth-order Runge-Kutta method [65], using to that end the coefficients appearing in Table 2.

The resulting absorbance-time plots corresponding to a couple of kinetic runs performed one in the initial absence of the autoinhibitor Fe(III) (Fig. 10, top) and the other in its presence (Fig. 10, bottom), all the other experimental conditions being the same, are shown. As can be observed, the simulations indicated that a reasonably good agreement between theory and experiment was reached also at $t > 0$.

Thus, it can be concluded that the experimental rate law obtained by application of the initial rate method, as well as the mechanism proposed to explain it, are both close approximations to the reality of this indeed complex free radical reaction.

References

1. Harman D (2006) Free radical theory of aging: an update increasing the functional lifespan. Ann N Y Acad Sci 1067:10 – 21
2. Boveris A (1998) Biochemistry of free radicals: from electrons to tissues. Medicina (B. Aires) 58:350 – 356
3. Valdez LB, Lores Arnaiz S, Bustamante J, Alvarez S, Costa LE, Boveris A (2000) Free radical chemistry in biological systems. Biol Res 3:65 – 70
4. Chan PH (2001) Reactive oxygen radicals in signaling and damage in the ischemic brain. J Cereb Blood Flow Metab 21:2 – 14

5. Perez-Benito JF (2006) A study of the cytochrome c-hydrogen peroxide reaction. Collect Czech Chem Commun 71:1588 – 1610
6. Sohal RS, Weindruch R (1996) Oxidative stress, caloric restriction, and aging. Science 273:59 – 63
7. Halliwell B, Gutteridge JMC (2015) Free radicals in biology and medicine. Oxford University Press, Oxford, p 440
8. Kwak MS, Rhee WJ, Lee YJ, Kim HS, Kim YH, Kwon MK, Shin JS (2021) Reactive oxygen species induce Cys106-mediated anti-parallel HMGB1 dimerization that protects against DNA damage. Redox Biol 40:101858
9. Ames BN (1983) Dietary carcinogens and anticarcinogens - Oxygen radicals and degenerative diseases. Science 221:1256 – 1264
10. Cortopassi G, Wang E (1995) Modeling the effects of age-related mtDNA mutation accumulation; complex I deficiency, superoxide and cell death. Biochim Biophys Acta 1271:171 – 176
11. Al-Ajlouni AM, Espenson JH, Bakac A (1993) Reaction of hydrogen peroxide with the oxochromium(IV) ion by hydride transfer. Inorg Chem 32:3162 – 3165
12. Winterbourn CC (2013) The biological chemistry of hydrogen peroxide. Methods Enzymol 528:3 – 25
13. Illes E, Patra SG, Marks V, Mizrahi A, Meyerstein D (2020) The Fe^{II}(citrate) Fenton reaction under physiological conditions. J Inorg Biochem 206:111018
14. Yu Z, Thompson Z, Behnke SL, Fenk KD, Huang D, Shafaat HS, Cowan JA (2020) Metalloglycosidase mimics: oxidative cleavage of saccharides promoted by multinuclear copper complexes under physiological conditions. Inorg Chem 59:11218 – 11222

15. Rush JD, Koppenol WH (1986) Oxidizing intermediates in the reaction of ferrous EDTA with hydrogen peroxide. J Biol Chem 261:6730 – 6733

16. Rush JD, Koppenol WH (1987) The reaction between ferrous polyaminocarboxylate complexes and hydrogen peroxide: an investigation of the reaction intermediates by stopped flow spectrophotometry. J Inorg Biochem 29:199 – 215

17. Rahhal S, Richter HW (1988) Reduction of hydrogen peroxide by the ferrous iron chelate of diethylenetriamine-N,N,N',N'',N''-pentaacetate. J Am Chem Soc 110:3126 – 3133

18. Masarwa M, Cohen H, Meyerstein D, Hickman DL, Bakac A, Espenson JH (1988) Reactions of low-valent transition-metal complexes with hydrogen peroxide. Are they "Fenton-like" or not? 1. The case of Cu^{+}_{aq} and Cr^{2+}_{aq}. J Am Chem Soc 110:4293 – 4297

19. Yamazaki I, Piette LH (1991) EPR spin-trapping study on the oxidizing species formed in the reaction of the ferrous ion with hydrogen peroxide. J Am Chem Soc 113:7588-7593

20. Sawyer DT, Kang C, Llobet A, Redman C (1993) Fenton reagents (1:1 $Fe^{II}L_x$/HOOH) react via [$L_xFe^{II}OOH(BH^{+})$] as hydroxylases (RH → ROH), not as generators of free hydroxyl radicals ($HO^{\bullet}$). J Am Chem Soc 115:5817 – 5818

21. Hage JP, Llobet A, Sawyer DT (1995) Aromatic hydroxylation by Fenton reagents {reactive intermediate [$L_x^{+}Fe^{III}OOH(BH^{+})$], not free hydroxyl radical ($HO^{\bullet}$)}. Bioorg Med Chem 3:1383 – 1388

22. Sawyer DT, Sobkowiak A, Matsushita T (1996) Metal [ML_x; M = Fe, Cu, Co, Mn]/hydroperoxide-induced activation of dioxygen for the oxygenation of hydrocarbons: oxygenated Fenton chemistry. Acc Chem Res 29:409 – 416

23. Kremer ML (1999) Mechanism of the Fenton reaction. Evidence for a new intermediate. Phys Chem Chem Phys 1:3595-–3605

24. Kremer ML (2003) The Fenton reaction. Dependence of the rate on pH. J Phys Chem A 107:1734–1741

25. Rachmilovich-Calis S, Masarwa A, Meyerstein N, Meyerstein D (2005) The Fenton reaction in aerated aqueous solutions revisited. Eur J Inorg Chem 2875–2880

26. Kremer ML (2017) Strong inhibition of the Fe^{3+} + H_2O_2 reaction by ethanol: evidence against the free radical theory. Prog React Kinet Mech 42:397–413

27. Walling C (1998) Intermediates in the reactions of Fenton type reagents. Acc Chem Res 31:155–157

28. Marusawa H, Ichikawa K, Narita N, Murakami H, Ito K, Tezuka T (2002) Hydroxyl radical as a strong electrophilic species. Bioorg Med Chem 10:2283–2290

29. Perez-Benito JF (2004) Iron(III)-hydrogen peroxide reaction: kinetic evidence of a hydroxyl-mediated chain mechanism. J Phys Chem A 108:4853–4858

30. Perez-Benito JF (2004) Reaction pathways in the decomposition of hydrogen peroxide catalyzed by copper(II). Inorg Biochem 98:430–438

31. Zeng Q, Wang X, Liu X, Huang L, Hu J, Chu R, Tolic N, Dong H (2020) Mutual interactions between reduced Fe-bearing clay minerals and humic acids under dark, oxygenated conditions: hydroxyl radical generation and humic acid transformation. Environ Sci Technol 54:15013–15023

32. Sun X, Gu X, Lyu, S (2021) The performance of chlorobenzene degradation in groundwater: comparison of hydrogen peroxide, nanoscale calcium peroxide and sodium percarbonate activated with ferrous iron. Water Sci Technol 83:344–357

33. Chen H, Fang C, Gao X, Jiang G, Wang X, Sun S, Wu W, Wu Z (2021) Sintering- and oxidation-resistant ultrasmall Cu(I)/(II) oxides supported on defect-rich mesoporous alumina microspheres boosting catalytic ozonation. J Colloid Interface Sci 581:964 – 978

34. Barb WG, Baxendale JH, George P, Hargrave KR (1955) Reactions of ferrous and ferric ions with hydrogen peroxide. III. Reactions in the presence of 2,2'-bipyridine. Trans Faraday Soc 51:935 – 946

35. Walling C, Kurz M, Schugar HJ (1970) The iron(III)-ethylenediaminetetraacetic acid-peroxide system. Inorg Chem 9:931 – 937

36. Walling C, Partch RE, Weil T (1975) Kinetics of the descomposition of hydrogen peroxide catalyzed by ferric ethylenediaminetetraacetate complex. Proc Nat Acad Sci 72:140 – 142

37. Francis KC, Cummins D, Oakes J (1985) Kinetic and structural investigations of [Fe^{III}(EDTA)]-[EDTA=Ethylenediaminetetra-acetate(4-) catalysed decomposition of hydrogen peroxide. J Chem Soc Dalton Trans 493 – 501

38. Amina, Si X, Wu K, Si Y, Yousaf B (2018) Synergistic effects and mechanisms of hydroxyl radical-mediated oxidative degradation of sulfamethoxazole by Fe(II)-EDTA catalyzed calcium peroxide: implications for remediation of antibiotic-contaminated water. Chem Eng J 353:80 – 91

39. Bray DG, Thompson RC (1994) Trace metal ion catalysis in the oxidation of $Fe(CN)_6^{4-}$ by H_2O_2. Inorg Chem 33:905 – 909

40. Karunakaran C, Muthukumaran B (1996) Kinetic evidence for peroxo complex formation in perborate or hydrogen peroxide oxidation of hexacyanoferrate(II). Pol J Chem 70:79 – 82

41. Kislenko VN, Oliinyk LP (2003) Kinetics of hydrogen peroxide decomposition in guaiacol solution, catalyzed by hexacyanoferrate(II). Russ J Gen Chem 73:114 – 118

42. Rabai G (1991) pH oscillation in the closed system of H_2O_2-$[Fe(CN)_6]^{4-}$-acetonitrile water. J Chem Soc, Chem Commun 1083 – 1084

43. Katafias A, Impert O, Kita P (2008) Hydrogen peroxide as a reductant of hexacyanoferrate(III) in alkaline solutions: kinetic studies. Transition Met Chem 33:1041 – 1046

44. Baxendale JH (1952) Decomposition of hydrogen peroxide by catalysts in homogeneous aqueous solution. Adv Catal 4:31 – 86

45. Domingo PI, Garcia B, Leal JM (1989) Acid-base behaviour of the ferricyanide ion in perchloric acid media. Spectrophotometric and kinetic study. Can J Chem 68:228 – 235

46. Perez-Benito JF, Arias C, Amat E (1995) A kinetic study of the reactions of cisplatin with biological thiols. New J Chem 19:1089 – 1094

47. Laidler KJ (1987) Chemical kinetics. Harper Collins, New York, p 30

48. Kuhn DD, Young TC (2005) Photolytic degradation of hexacyanoferrate(II) in aqueous media: the determination of the degradation kinetics. Chemosphere 60:1222 – 1230

49. Bell S, Foster G, Fuller MW, Hughes D, Le Brocq KMF, Leslie E, Wilson IR (1986) Spectrophotometric measurement of rates of hexacyanoferrate(III) reactions. Int J Chem Kinet 18:651 – 653

50. Perez-Benito JF, Arias C, Brillas E (1990) Comment on monitoring of hexacyanoferrate(III) reactions by spectrophotometric methods. Int J Chem Kinet 22:95 – 97

51. Bruice PY (2016) Organic chemistry. Pearson, Upper Saddle River, New Jersey, p 404

52. Behar D (1974) Pulse radiolysis study of aqueous hydrogen cyanide and cyanide solutions. J Phys Chem 78:2660 – 2663

53. Luo L, Yao Y, Gong F, Huang ZF, Lu WY, Chen WX, Zhang L (2016) Drastic enhancement on Fenton oxidation of organic contaminants by accelerating Fe(II)/Fe(III) cycle with L-cysteine. RSC Adv 6:47661 – 47668

54. Sawyer DT, Valentine JS (1981) How super is superoxide?. Acc Chem Res 14:393 – 400

55. Barb WG, Baxendale JH, George P, Hargrave KR (1951) Reactions of ferrous and ferric ions with hydrogen peroxide. Part I: The ferrous ion reaction. Trans Faraday Soc 47:462 – 500

56. Barb WG, Baxendale JH, George P, Hargrave KR (1951) Reactions of ferrous and ferric ions with hydrogen peroxide. Part II: The ferric ion reaction. Trans Faraday Soc 47:591 – 616

57. Weinstein J, Bielski BHJ (1979) Kinetics of the interaction of HO_2 and O_2^- radicals with hydrogen peroxide. The Haber-Weiss reaction. J Am Chem Soc 101:58 – 62

58. Rush JD, Bielski BHJ (1985) Pulse radiolytic studies of the reaction of perhydroxyl/superoxide HO_2/O_2^- with Fe(II)/Fe(III) ions. The reactivity of HO_2/O_2^- with ferric ions and its implication on the occurrence of the Haber-Weiss reaction. J Phys Chem 89:5062 – 5066

59. Wilkinson F (1980) Chemical kinetics and reaction mechanisms. Van Nostrand Reinhold, New York, pp 42 – 44

60. Perez-Benito JF (2017) Some considerations on the fundamentals of chemical kinetics: steady state, quasi-equilibrium, and transition state theory. J Chem Educ 94:1238 – 1246

61. Wang J, Wang S (2021) Effect of inorganic anions on the performance of advanced oxidation processes for degradation of organic contaminants. Chem Eng J 411:128392
62. Han M, Jafarikojour M, Hamachi M, Mohseni M (2021) The impact of chloride and chlorine radical on nitrite formation during vacuum photolysis of water. Sci Total Environ 760:143325
63. Xu HB, Zhu YP, Cui DJ, Du MR, Wang JQ, Ma RN, Jiao Z (2019) Evaluating the roles of OH radicals, H_2O_2, ORP and pH in the inactivation of yeast on a tissue model by surface micro-discharge plasma. J Phys D 52:395201
64. Krewing M, Schubert B, Bandow JE (2020) A dielectric barrier discharge plasma degrades proteins to peptides by cleaving the peptide bond. Plasma Chem Plasma Process 40:685-696
65. Espenson JH (1995) Chemical kinetics and reaction mechanisms. McGraw-Hill, New York, p 113 – 115

Table 1 Arrhenius and Eyring activation parameters[a]

Activation parameter	Experimental value
ln (A/s^{-1})[b]	10.6 ± 1.1
E_a / kJ mol^{-1}[c]	28.9 ± 2.7
$\Delta H^{o}_{\ddagger}$ / kJ mol^{-1}[d]	26.4 ± 2.7
$\Delta S^{o}_{\ddagger}$ / J K^{-1} mol^{-1}[e]	− 165 ± 9

[a] $[K_4Fe(CN)_6]_o = 1.97 \times 10^{-4}$ M, $[H_2O_2]_o = 1.57 \times 10^{-2}$ M, $[KH_2PO_4] = 7.20 \times 10^{-2}$ M, pH 4.56, 15.0 – 35.0 °C

[b] Arrhenius pre-exponential factor (logarithmic form)

[c] Activation energy

[d] Activation enthalpy

[e] Activation entropy

Table 2 Experimental values of the rate law parameters[a]

Rate law parameter	Experimental value	Units
k_{I}	0.276	$M^{-1}\ s^{-1}$
k_{II}	13.9	$M^{-2}\ s^{-1}$
k_{III}	9.79×10^{3}	$M^{-2}\ s^{-1}$
k_{IV}	84.2	$M^{-1}\ s^{-1}$
k_{V}	1.83×10^{4}	M^{-1}
k_{VI}	3.87×10^{4}	M^{-1}
k_{VII}	1.36×10^{3}	M^{-1}
k_{VIII}	64.4	M^{-1}

[a] $[Fe(II)]_o = (1.97 - 9.85) \times 10^{-4}$ M, $[H_2O_2]_o = (0.78 - 3.92) \times 10^{-2}$ M, $[Fe(III)]_o = (0.00 - 7.87) \times 10^{-4}$ M, $[KH_2PO_4] = 7.20 \times 10^{-2}$ M, pH 4.56, 25.0 ^oC

Table 3 Mathematical identities for the parameters involved in the experimental rate law as inferred from the proposed mechanism (α_h is the hydrolysis degree, $0 < \alpha_h < 1$).

Rate law parameter	Mechanism parameters
k_I	$\dfrac{\alpha_h k_5\left(k_7 K_{11} k_{17} + 2 k_8 k_{15} [H^+]_o [O_2]_o\right)}{K_{11} k_{17}\left(k_{-5} [H_2O]_o + k_8 [O_2]_o\right)}$
k_{II}	$\dfrac{2 \alpha_h k_5 k_7 k_{15} [H^+]_o}{K_{11} k_{17}\left(k_{-5} [H_2O]_o + k_8 [O_2]_o\right)}$
k_{III}	$\dfrac{2 \alpha_h k_5 k_7 k_{13} [H^+]_o}{K_{11} k_{17}\left(k_{-5} [H_2O]_o + k_8 [O_2]_o\right)}$
k_{IV}	$\dfrac{2 \alpha_h k_5 k_8 k_{13} [H^+]_o [O_2]_o}{K_{11} k_{17}\left(k_{-5} [H_2O]_o + k_8 [O_2]_o\right)}$
k_V	$\dfrac{k_{13} [H^+]_o}{K_{11} k_{17}}$
k_{VI}	$\dfrac{k_{14}}{k_{17}}$
k_{VII}	$\dfrac{\alpha_h k_6}{k_{-5} [H_2O]_o + k_8 [O_2]_o}$
k_{VIII}	$\dfrac{k_7}{k_{-5} [H_2O]_o + k_8 [O_2]_o}$

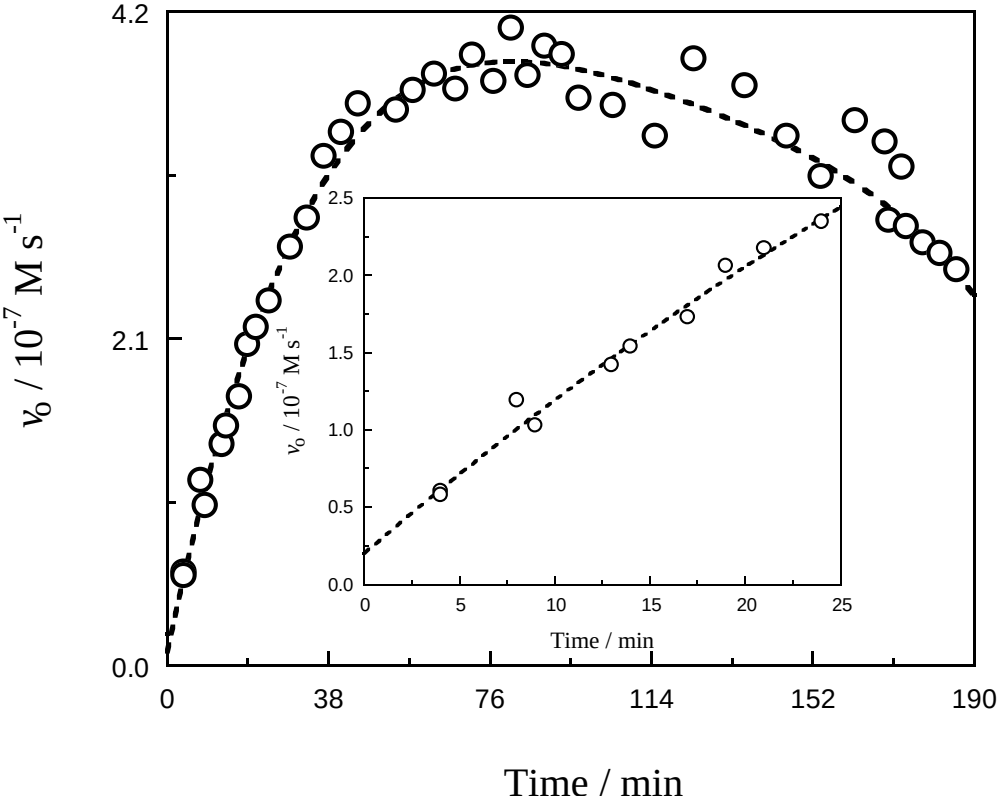

Fig. 1 Dependence of the initial rate on the time elapsed after preparation of the Fe(II) stock solution (4.94×10^{-3} M). Inset: detail showing the extrapolation at $t = 0$. $[K_4Fe(CN)_6]_o = 3.95 \times 10^{-4}$ M, $[H_2O_2]_o = 9.79 \times 10^{-3}$ M, $[KH_2PO_4]_o = [K_2HPO_4]_o = 7.20 \times 10^{-2}$ M, pH 6.79, 25.0 ºC. The dashed lines are the best fits to show the experimental trends.

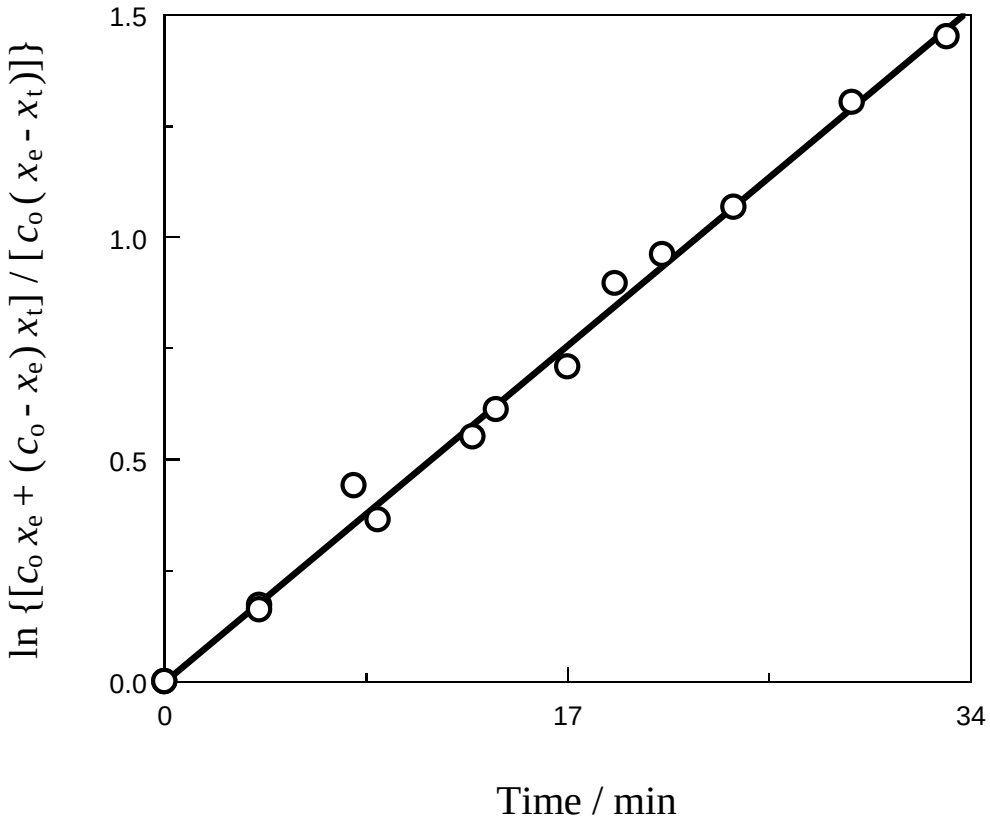

Fig. 2 Kinetic plot (r = 0.9967) corresponding to the integrated rate law for the hydrolysis of $K_4[Fe(CN)_6]$ (4.94×10^{-3} M) in the absence of additives at 25.0 ºC

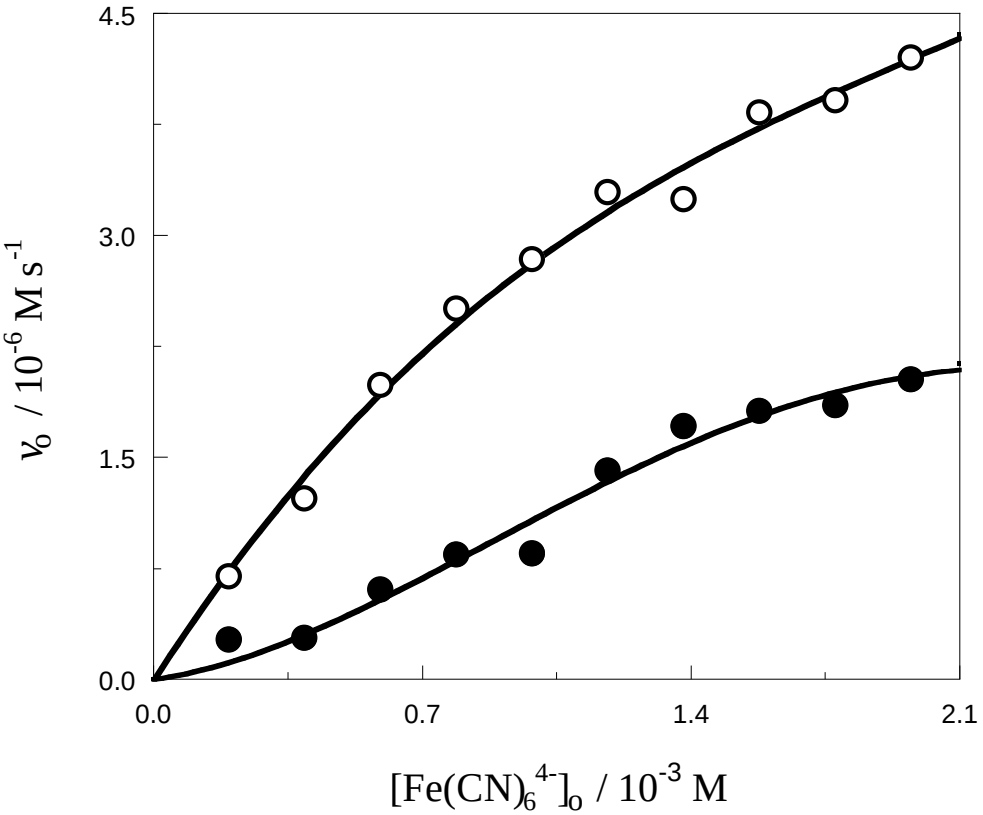

Fig. 3 Dependences of the initial rate on the initial concentration of hexacyanoferrate(II) ion at $[H_2O_2] = 3.13 \times 10^{-3}$ M, $[KH_2PO_4] = [K_2HPO_4] = 7.20 \times 10^{-2}$ M, pH 6.79 × 0.02 and 25.0 ºC when the $K_4[Fe(CN)_6]$ stock solution was prepared and thermostated under either ordinary laboratory-illumination conditions (empty circles) or semi-darkness conditions (filled circles)

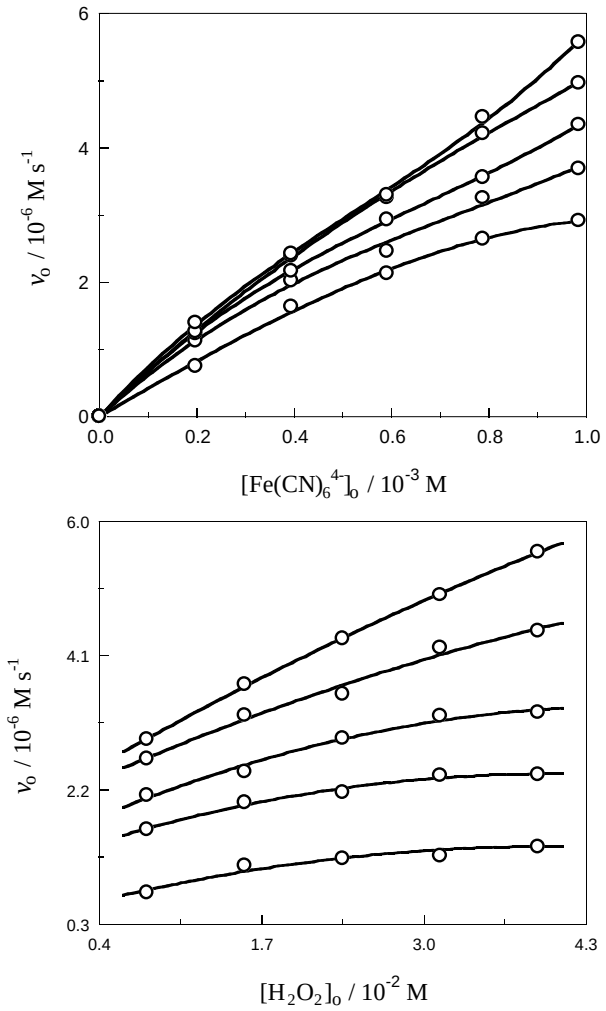

Fig. 4 Initial rate of the oxidation of hexacyanoferrate(II) ion by hydrogen peroxide as a function of the initial concentrations of either Fe(II) (top) or H_2O_2 (bottom) in the presence of KH_2PO_4 (7.20×10^{-2} M) at pH 4.56 and 25.0 ºC. Top: $[H_2O_2]_o$ = 0.78, 1.57, 2.35, 3.13 and 3.92×10^{-2} M (in ascending order). Botom: $[Fe(II)]_o$ = 1.97, 3.94, 5.91, 7.88 and 9.85×10^{-4} M (in ascending order)

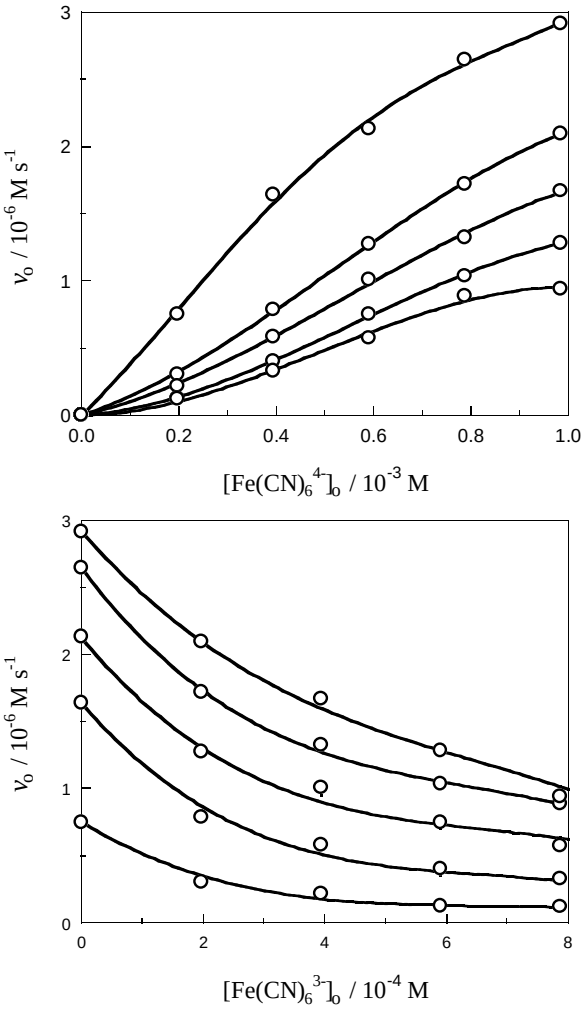

Fig. 5 Initial rate of the oxidation of hexacyanoferrate(II) ion by hydrogen peroxide (7.83×10^{-3} M) as a function of the initial concentrations of either Fe(II) (top) or Fe(III) (bottom) in the presence of KH_2PO_4 (7.20×10^{-2} M) at pH 4.56 and 25.0 ^{o}C. Top: $[Fe(III)]_o$ = 0.00, 1.97, 3.94, 5.90 and 7.87×10^{-4} M (in descending order). Bottom: $[Fe(II)]_o$ = 1.97, 3.94, 5.91, 7.88 and 9.85×10^{-4} M (in ascending order)

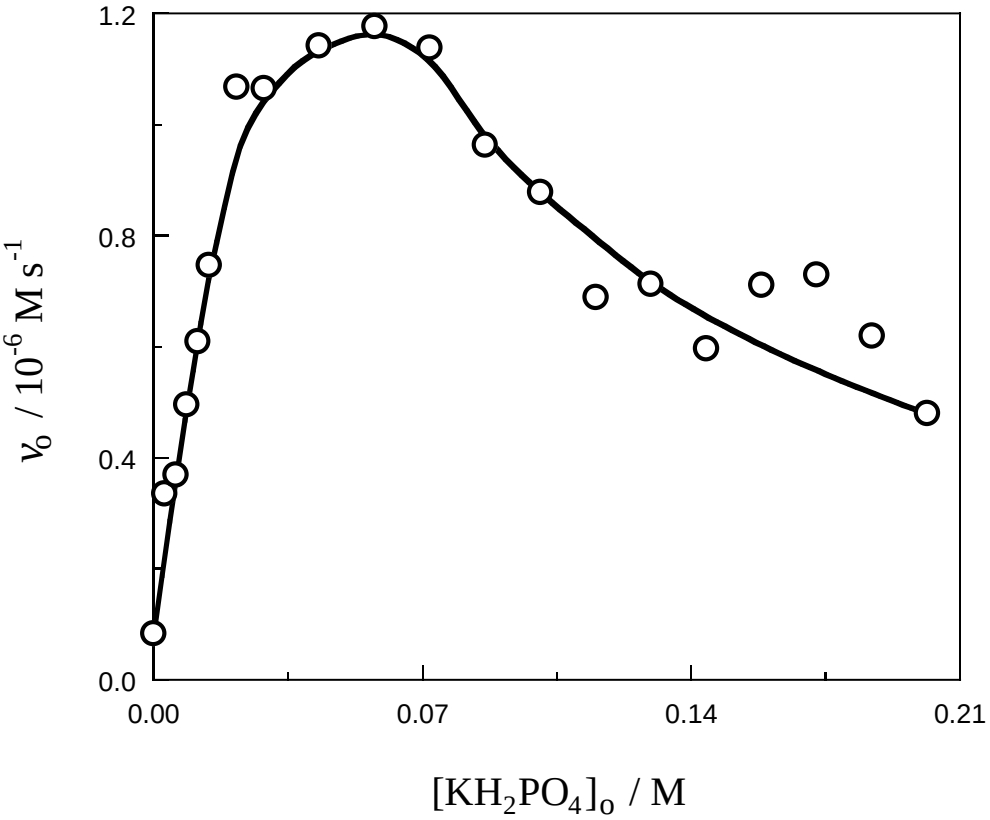

Fig. 6 Initial rate of the oxidation of hexacyanoferrate(II) ion (1.97×10^{-4} M) by hydrogen peroxide (7.83×10^{-3} M) as a function of the KH_2PO_4 initial concentration at pH 4.36 – 6.65 and 25.0 ºC

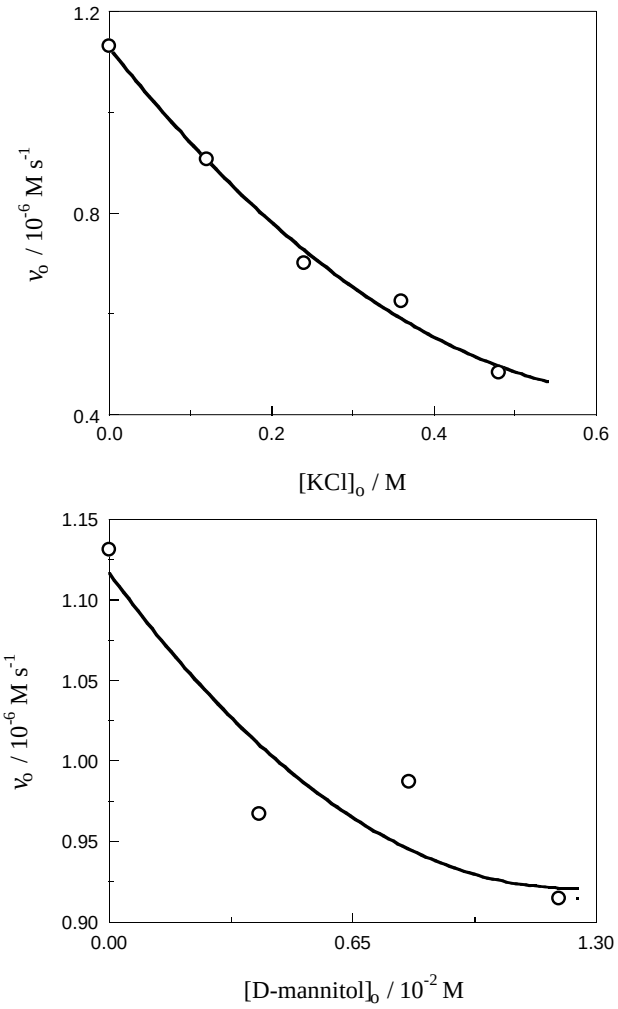

Fig. 7 Initial rate of the oxidation of hexacyanoferrate(II) ion (1.97×10^{-4} M) by hydrogen peroxide (1.57×10^{-2} M) as a function of the initial concentrations of either potassium chloride (top) or D-mannitol (bottom) in the presence of KH_2PO_4 (7.20×10^{-2} M) at pH 4.56 and 25.0 ^{o}C

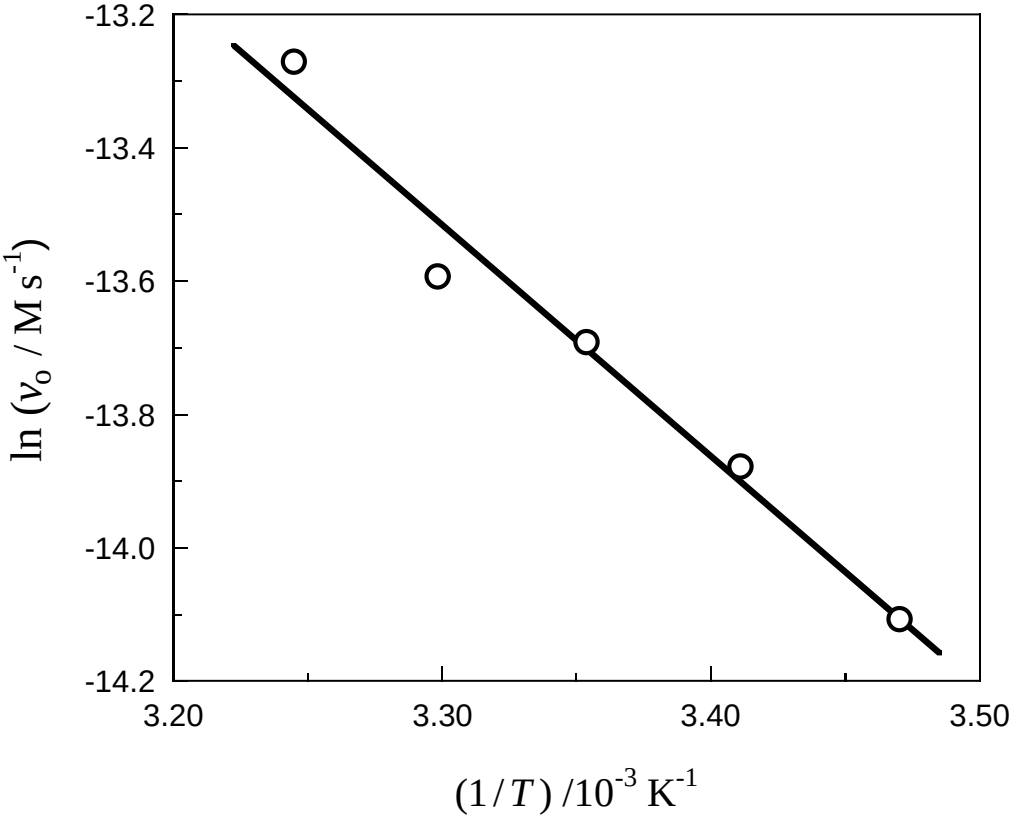

Fig. 8 Arrhenius plot (r = 0.9867) for the oxidation of hexacyanoferrate(II) ion (1.97×10^{-4} M) by hydrogen peroxide (1.57×10^{-2} M) in the presence of KH_2PO_4 (7.20×10^{-2} M) at pH 4.56 and 15.0 – 35.0 ^{o}C

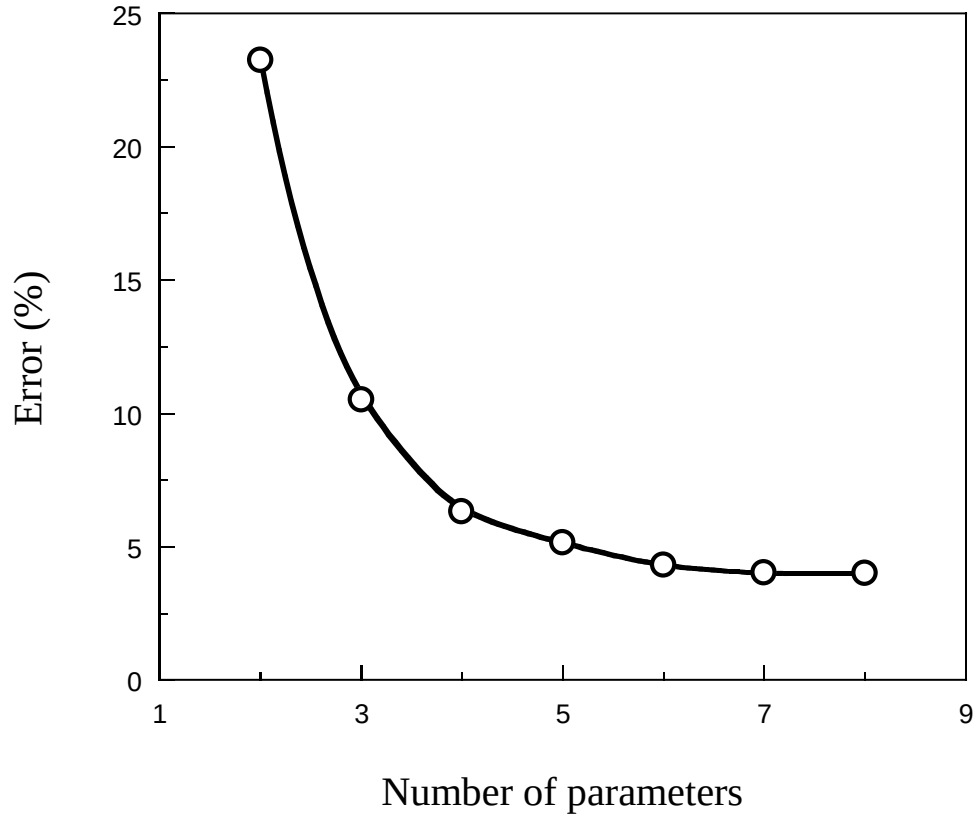

Fig. 9 Percent error of the predictions based on a trial rate law as compared with 45 values of the initial rate for the oxidation of hexacyanoferrate(II) ion by hydrogen peroxide as a function of the number of parameters involved in the law. Variable experimental conditions: $[Fe(II)]_o = (1.97 - 9.85) \times 10^{-4}$ M, $[H_2O_2]_o = (0.78 - 3.92) \times 10^{-2}$ M and $[Fe(III)]_o = 0.00 - 7.87 \times 10^{-4}$ M. Constant experimental conditions: $[KH_2PO_4]_o = 7.20 \times 10^{-2}$ M, pH 4.56 and 25.0 ºC

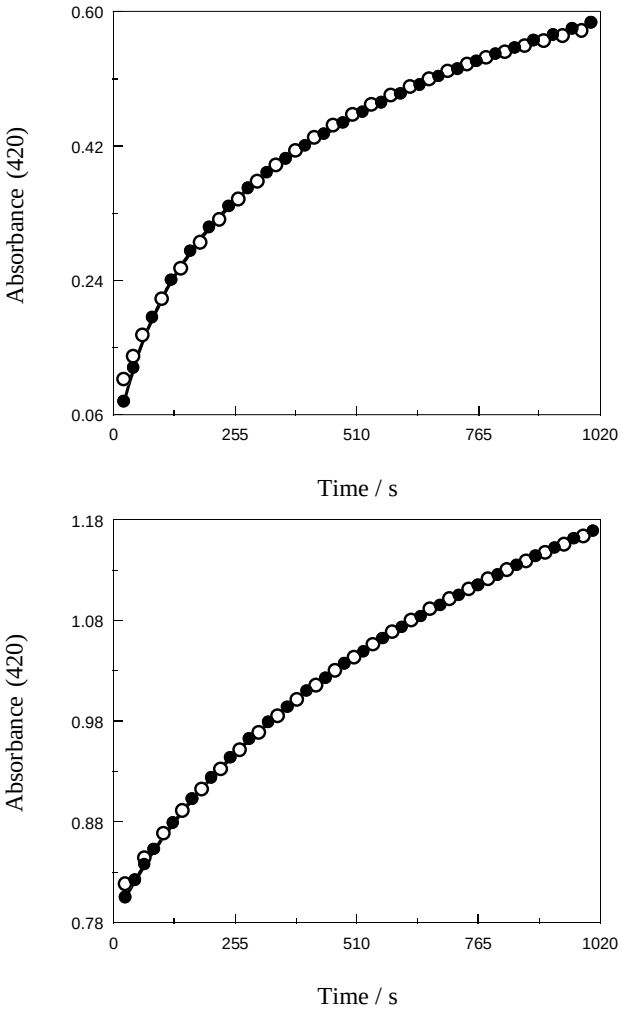

Fig. 10 Absorbance at 420 nm as a function of time at $[Fe(III)]_o = 0$ (left, average deviation: ΔA = ± 0.0037) and 7.87×10^{-4} M (right, average deviation: ΔA = ± 0.0016), showing the experimental (filled circles) and simulated (empty circles) values. $[K_4Fe(CN)_6]_o = 9.85 \times 10^{-4}$ M, $[H_2O_2]_o = 7.83 \times 10^{-3}$ M, $[KH_2PO_4]_o = 7.20 \times 10^{-2}$ M, pH 4.56, 25.0 ºC

$$v_o = \frac{k_I [Fe^{II}]_o^2 [H_2O_2]_o}{[Fe^{II}]_o + k_{II} [Fe^{III}]_o}$$

$N = 2$ ↓ Error = 23.26 %

$$v_o = \frac{\left(k_I [H_2O_2]_o + k_{II} [Fe^{II}]_o\right) [Fe^{II}]_o}{[Fe^{II}]_o + k_{III} [Fe^{III}]_o}$$

$N = 3$ ↓ Error = 10.51 %

$$v_o = \frac{\left(k_I + k_{II} [Fe^{II}]_o\right) [Fe^{II}]_o [H_2O_2]_o}{\left([Fe^{II}]_o + k_{III} [Fe^{III}]_o\right)\left(1 + k_{IV} [H_2O_2]_o\right)}$$

$N = 4$ ↓ Error = 6.32 %

$$v_o = \frac{\left(k_I [H_2O_2]_o + k_{II} [Fe^{II}]_o\right) [Fe^{II}]_o [H_2O_2]_o}{\left([Fe^{II}]_o + k_{III} [Fe^{III}]_o + k_{IV} [H_2O_2]_o\right)\left(1 + k_V [H_2O_2]_o\right)}$$

$N = 5$ ↓ Error = 5.15 %

$$v_o = \frac{\left(k_I [H_2O_2]_o + k_{II} [Fe^{II}]_o\right) [Fe^{II}]_o [H_2O_2]_o}{\left(1 + k_{III} [Fe^{II}]_o + k_{IV} [Fe^{III}]_o\right)\left(1 + k_V [Fe^{II}]_o + k_{VI} [H_2O_2]_o\right)}$$

$N = 6$ ↓ Error = 4.31 %

$$v_o = \frac{\left(k_I + k_{II} [Fe^{II}]_o\right) [Fe^{II}]_o [H_2O_2]_o + k_{III} [Fe^{II}]_o^2}{\left(1 + k_{IV} [Fe^{II}]_o + k_V [Fe^{III}]_o\right)\left(1 + k_{VI} [Fe^{II}]_o + k_{VII} [H_2O_2]_o\right)}$$

$N = 7$ ↓ Error = 4.01 %

$$v_o = \frac{\left(k_I + k_{II} [H_2O_2]_o + k_{III} [Fe^{II}]_o\right) [Fe^{II}]_o [H_2O_2]_o + k_{IV} [Fe^{II}]_o^2}{\left(1 + k_V [Fe^{II}]_o + k_{VI} [Fe^{III}]_o\right)\left(1 + k_{VII} [Fe^{II}]_o + k_{VIII} [H_2O_2]_o\right)}$$

$N = 8$ ↔ Error = 4.00 %

Scheme 1 Flow chart with the best trial rate law for each number of parameters (N) indicating the corresponding percent error with respect to the initial rate experimental values